Available online at www.sciencedirect.com
ScienceDirect
Bioorganic & Medicinal Chemistry 16 (2008) 3878–3886
Bioorganic & Medicinal Chemistry

A spectroscopy approach for the study of the interactions of bioactive vanadium species with bovine serum albumin

Evelina G. Ferrer,[a,*] Alejandra Bosch,[b] Osvaldo Yantorno[b] and Enrique J. Baran[a]

[a]*Centro de Química Inorgánica (CEQUINOR, CONICET/UNLP), Facultad de Ciencias Exactas, Universidad Nacional de La Plata, C.C.962, 1900 La Plata, Argentina*
[b]*Centro de Investigación y Desarrollo de Fermentaciones Industriales (CINDEFI, CONICET/UNLP), Facultad de Ciencias Exactas, Universidad Nacional de La Plata, 1900 La Plata, Argentina*

Received 26 November 2007; revised 11 January 2008; accepted 23 January 2008
Available online 6 February 2008

Abstract—The interest in biological functions (benefits or toxics effects) of vanadium species has grown enormously in recent years. In this work, different spectroscopic methods were applied to study the effects of the interaction of vanadyl and vanadate species with bovine serum albumin (BSA), considered as the most abundant plasma protein. UV–Vis, Fourier transform infrared (FT-IR), and FT-Raman spectroscopies were used to investigate changes in secondary and tertiary structures of BSA induced by the binding of oxovanadium(IV) and vanadate(V) species (VO^{2+} and VO_3^-, respectively). Correlations between the metal ion binding mode, protein conformational transitions, and structural variations were established.
Published by Elsevier Ltd.

1. Introduction

Bovine serum albumin (BSA) is the most abundant protein plasma. It is a multiple function protein, though its most outstanding property is its ability to bind reversibly a huge amount of compounds. BSA is the principal carrier of fatty acids, metabolic products, regulatory mediators, and nutrients.[1–5] Besides, it binds and neutralizes endogenous or exogenous toxins by means of hydrogen bonding,[6] hydrophobic, electrostatic, and metal interactions.[7] It has been reported that BSA forms covalent adducts with various metals such as Cu(II), Ni(II), Hg(II), Ag(II), and Au(I). Particularly, studies on the interaction of BSA with Cu(II) and Ni(II) reported for bovine, human, and rat serum albumins (BSA, HSA, and RSA, respectively), account for the existence of a high-affinity binding site called amino terminal Cu(II)- and Ni(II)-(ATCUN) motif.[8] In these cases metal binding to this site occurs through the interaction with nitrogen atoms derived from NH_2 groups, as imidazole group of histidine and different peptide residues.

Vanadium is a biologically ultramicrotrace transition metal which can be found both in anionic and cationic forms with oxidation states ranging from −1 to +5 (I–V).[9–11] The cationic forms of vanadium complexes with oxidation state +4 (IV) have been shown to modulate the cellular redox potential, regulate enzymatic phosphorylation, and exert pleiotrophic effects in multiple biological systems by catalyzing the generation of reactive oxygen species (ROS) in cellular and cell-free systems.[12–14] Vanadium species are present in several proteins including *bromoperoxidase* and *nitrogenase* being essential for their catalytic activity.[6–8,15–21] Moreover, the ability of vanadium to assume various oxidation states contributes to the versatility of this metal in biological systems and allows its interaction with different biomolecules.[8,22,23] It was demonstrated by electron paramagnetic resonance (EPR) and angle-selected electron nuclear double resonance (ENDOR) that both inorganic salts and organic chelates of VO^{2+} cation have insulin-mimetic effects and are able to participate in glucose uptake and metabolism. These insulin-like properties of organic chelates of VO^{2+} might be dependent on adduct formation with BSA and possibly with other serum transport proteins.[15]

Different analytical and spectroscopic methods (ESR: electron spin resonance spectroscopy, UV–Vis–DRS; DRS: diffuse reflectance spectroscopy) have been used

Keywords: Vanadium species; Bovine serum albumin (BSA); Infrared spectroscopy (FT-IR/ATR); Raman spectroscopy (FT-Raman).
* Corresponding author. Tel./fax: +54 0221 4259485; e-mail: evelina@quimica.unlp.edu.ar

0968-0896/$ - see front matter Published by Elsevier Ltd.
doi:10.1016/j.bmc.2008.01.060

to study the interaction of vanadium species with HSA, BSA, or with transferrin protein. Nevertheless, the mechanisms by which they interact with biological molecules have not been clearly elucidated yet.[21,24–27] In recent years, Fourier transform infrared spectroscopy (FT-IR) and FT-Raman spectroscopy have been widely used as a tool to monitor chemical structure changes of polypeptides and proteins, particularly they were applied to determine protein secondary structure modifications in both aqueous and non-aqueous solutions.[28–34] Since non-polar groups give intense absorbances in Raman spectra, and polar groups cause high-absorption peaks in FT-IR spectroscopy; the use of both spectroscopic techniques in a complementary fashion, can provide important and complete information.[35] FT-IR spectroscopy has the advantage of giving higher signal-to-noise ratio, while FT-Raman can provide additional information on the tertiary structure of proteins and the microenvironment of protein side chains.[29,30] An important difference to remark between these techniques is that the O–H stretching vibration is very strong in IR, but very weak in Raman spectra. For this reason, water is practically 'invisible' in Raman spectroscopy, while it dominates the IR spectrum, if present. Due to this fact, Raman scattering has the advantage of allowing the study of protein structure in situ. Both techniques in cooperation have enabled the understanding and monitoring of structural changes produced in proteins under the influence of diverse environmental conditions or different processes such as mixing, aeration, thermal treatments, aggregation and gelation, buffer conditions, incorporation of chaotropic salts, protein structure perturbants (dithiothreitol, ethylene glycol, dodecylsulfate), and coordination of ligands such as metals and organometallic compounds.[28,33,35–39] IR spectroscopy of biological samples has been widely implemented with the attenuated total reflection (ATR) technique.[40,41] For FT-IR/ATR measurements, the sample is placed on the surface of a trapezoidal-shaped IR-transparent crystal. The IR beam is guided through the crystal in such a way that some total reflections take place at the surface. The penetration depth of the IR radiation in this arrangement is of a few micrometers. Therefore, the IR spectrum obtained contains only information about the very thin layer of the sample that is in close proximity to the surface of the crystal. Thus, by means of this technique it is possible to obtain a spectrum of a protein in H_2O or buffer solution without much interference from IR absorption of the bulk water.[33]

In this paper, we investigate the ability of vanadate and vanadyl ions to produce conformational changes in native BSA in Tris–HCl buffer solutions at physiological pH. For these purposes, FT-IR/ATR, FT-Raman, and UV–Vis spectroscopic techniques have been used. A quantitative analysis is provided of each conformational component such as α-helix, β-sheet, turns, and random coil structures for BSA, and the corresponding vanadium complexes. Our work attempts to give the basis for the understanding of BSA/vanadium interactions which might provide significant insights into structural features, critical to biological functions. Since most studies of metals binding to proteins focus on the metal coordination and not metal-induced perturbations of the protein structure, this study could serve as an example of complementary data that could be obtained when the binding of metal ions to proteins is studied.

2. Results and discussion

2.1. FTIR and UV–Vis spectroscopies

Amide I and Amide II bands (1700–1500 cm^{-1}) of IR spectra have been extensively used in the characterization of chemical composition and conformational studies of proteins. Particularly, Amide I (1690–1620 cm^{-1}) reflects an almost pure vibrational character, since it consists mainly of the carbonyl stretching vibration mode of the peptide bond. Therefore, it has a well-recognized potential in protein secondary structure studies.[28,34,42,43] To test whether the interaction of BSA with vanadium salts produces conformational changes in the native BSA protein, Amide I and II bands of FT-IR/ATR spectra of this protein and their vanadium complexes were analyzed. The main spectral features of native BSA are characterized by a strong Amide I band at 1657 cm^{-1} and an Amide II absorption band at 1541 cm^{-1}. The location of these bands (Fig. 1) is indicating that BSA secondary structure is dominated, as it has previously been reported, by α-helix conformation.[33,34,44–46] When we studied the interaction of vanadium species like oxovanadium(IV) or vanadate(V) (VO^{2+} and VO_3^- with native BSA by FT-IR/ATR spectroscopy, we observed that low concentrations (0.005 and 0.05 mM) of these species did not produce significant changes on BSA structure (data not shown). The FT-IR spectroscopy studies revealed that under our

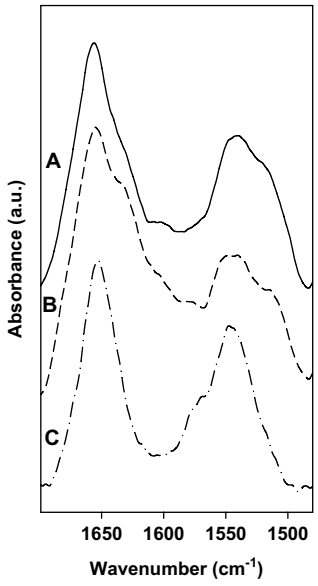

Figure 1. FT-IR spectra showing Amide I and Amide II bands of free BSA (A), and the vanadium complexes BSA/VO^{2+} (B), and BSA/VO_3^- (C), obtained after 1 h-incubation time in Tris–HCl buffer, pH 7.4, solution.

experimental conditions, vanadium concentrations should be equal or higher than 0.5 mM to produce detectable spectral changes associated to BSA secondary structure. Incubations with oxovanadium(IV) and vanadate(V) species at this concentration and under the conditions indicated in methods, produced small shifts of the typical 1657 cm^{-1} band present in BSA spectrum toward lower frequencies (1655 and 1653 cm^{-1} for V(IV) and V(V), respectively) (Fig. 1). Furthermore, Amide II band at 1542 cm^{-1} in native BSA shifted to 1547 cm^{-1} for both species. Besides the shoulder observed in BSA spectrum at 1521 cm^{-1} appeared at 1514 cm^{-1} for V(IV) complexes and its intensity vanished for V(V) ion compounds.

Second derivative of BSA in Tris–HCl buffer solution and BSA vanadium complexes FT-IR spectra were analyzed in order to perform a quantitative analysis of the corresponding secondary structures in Amide I region.[28,47] Second derivative spectra of free BSA showed a strong peak at 1657 cm^{-1}, which is assigned to α-helix, and other peaks at 1681, 1674, 1639, 1630, and 1619 cm^{-1} corresponding to β-antiparallel, turn, random coil, solvated helical structure, and β-sheet, respectively[33,42,46] (Fig. 2A). These frequencies were used as initial input parameters for the curve-fitting procedure. The secondary structure of native BSA obtained by this methodology is indicated in Table 1. The percentages of the different secondary structure elements obtained were in agreement with several previously reported studies, using different techniques such as Raman spectroscopy,[48] circular dichroism,[6] and X-ray crystallographic studies[45] in which a high percentage of α-helix conformation in the native protein was reported. A quantitative analysis of the secondary structure was performed with spectra of vanadium complexes using the same analytical procedure. Figure 2B shows BSA/VO^{2+} second derivative spectra which displayed six minimums in Amide I region at 1678, 1666, 1655, 1642, and 1632 and 1623 cm^{-1}, assigned to β-antiparallel, turn, α-helix, random, solvated helix,

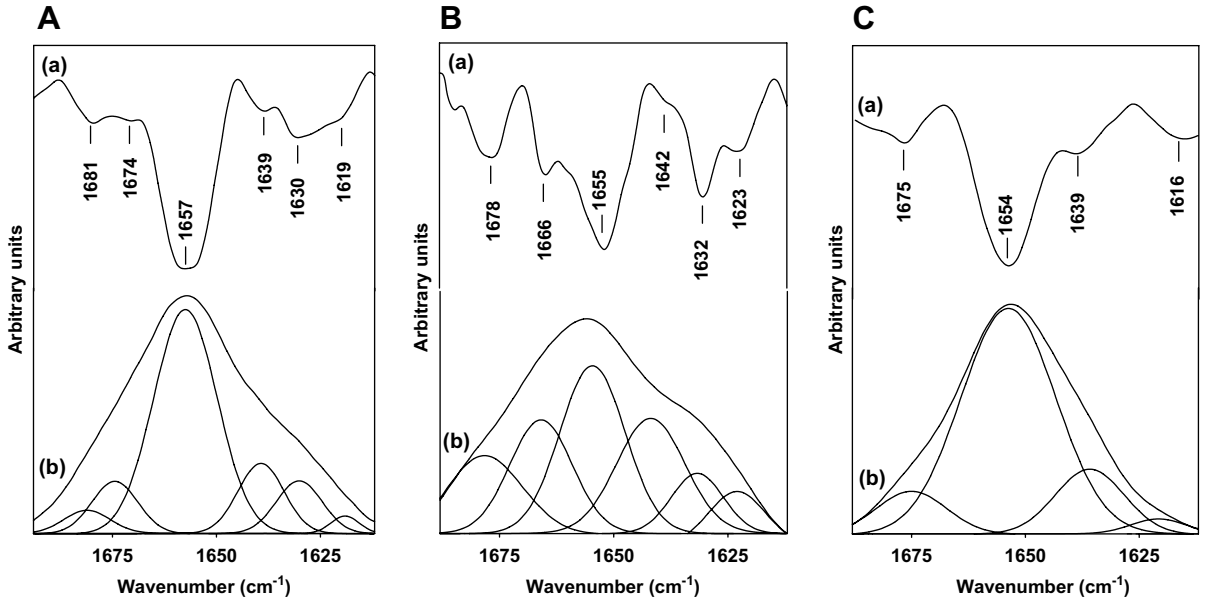

Figure 2. Second derivative (a) and original FT-IR/ATR spectra in Amide I region (b) of: (A) free BSA (2% w/v in Tris–HCl buffer solution), (B) BSA/VO^{2+} complex ([BSA] = 2% w/v, [VO^{2+}] = 0.5 mM in Tris–HCl buffer solution), (C) BSA/VO_3^- complex ([BSA] = 2% w/v, [VO_3^-] = 0.5 mM in Tris–HCl buffer solution. The secondary structure determination by curve-fitting procedure is indicated.

Table 1. FT-IR/ATR determination of secondary structure percentages of native BSA and its oxovanadium(IV) and vanadate(V) complexes in Tris–HCl buffer solution[a]

Amide I components[b]	BSA		BSA/VO^{2+}	BSA/VO_3^-
	FTIR	CD[c]	FTIR	FTIR
β-Antiparallel (1675–1695 cm^{-1})	4.45 ± 0.08	5	16.47 ± 0.79	10.21 ± 0.39
Turns (1666–1673 cm^{-1})	10.12 ± 0.48	13	18.55 ± 0.80	Not detected
α-Helix (1650–1658 cm^{-1})	59.76 ± 0.90	60	28.67 ± 0.86	72.12 ± 3.6
Random coil (1637–1645 cm^{-1})	13.45 ± 0.06	23	20.46 ± 0.61	15.10 ± 0.60
Solvated helix (1625–1637 cm^{-1})	10.14 ± 0.30		8.20 ± 0.20	Not detected
β-Sheets (1613–1625 cm^{-1})	2.08 ± 0.07		7.63 ± 0.30	2.70 ± 0.08

[a] BSA/VO^{2+} and BSA/VO_3^- complexes were obtained incubating [VO^{2+}] = 0.5 mM and [VO_3^-] = 0.5 mM with BSA (2% w/v) for 1 h at room temperature. Data represent average obtained from three independent replicates, standard error is indicated.

[b] Band assignment was performed taking into account Refs. 33, 42, and 46.

[c] Ref. 6.

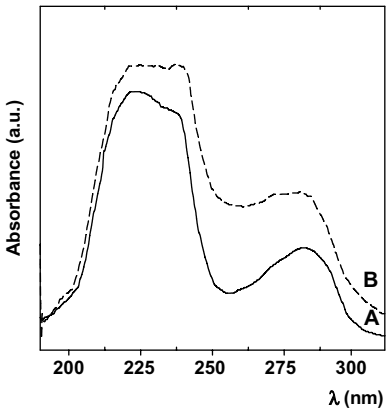

Figure 3. Electronic spectra of (A) free BSA (2% w/v in Tris–HCl buffer solution) and (B) BSA/VO^{2+} complex ([BSA] = 2% w/v, [VO^{2+}] = 0.5 mM in Tris–HCl buffer solution).

and β-sheet, respectively.[28,42,46] The curve-fitting procedure based on these second derivative spectra indicated that the α-helix content decreased to 28.67%, whereas β-structures (antiparallel and β-sheet), turns, and random coil structures increased as it is shown in Table 1. The drastic reduction observed in α-helix conformation and the significant enhancement in disordered structures and β conformations in relation to BSA native structure, are consistent with the hypothesis of the existence of a strong interaction between vanadyl (VO^{2+}) species and BSA. A similar behavior was reported for the interaction of BSA with metal cations as Cd(II), Hg(II), and Pb(II).[49,50] This significant interaction of vanadyl(IV) ions with BSA was also displayed in the UV–Vis spectra (Fig. 3). In our experiments, UV–Vis spectra of BSA solutions showed the two typical peaks at 200 and 280 nm assigned to peptide bond and aromatic amino acid side chains (phenylalanine, tryptophan, histidine, and tyrosine), respectively,[51] UV–Vis BSA/VO^{2+} spectra confirmed FT-IR spectroscopy results showing a significant intensity increment in 280 nm band (1.20 ± 0.03 in the BSA to 1.85 ± 0.04 in BSA/VO^{2+} complex), that could be due to a higher exposure of aromatic amino acid residues probably produced by an enhancement of unfolding in the protein (data not shown). Besides, the UV–Vis oxovanadium(IV) BSA complexes derivative spectra presented two maximum absorption bands: a strong one at 794 nm (band I) that could be assigned to $3d_{xy} \rightarrow 3d_{xz}$ ($b_2 \rightarrow e$) and a second band at 526 nm (band II) assigned to the $3d_{xy} \rightarrow 3d_{x_2-y_2}$ ($b_2 \rightarrow b_1$) d–d transition, according to the scheme of Ballhausen and Grey.[52] The band positions are similar to those obtained for amino acids/VO^{2+} systems, which correspond to coordination modes involving N and O atoms.[53] The interaction through oxygen atoms from terminal residues has also been suggested for Cu(II), Co(II), and Ni(II).[54] The observation that BSA could interact via N donors to positive charged ions is in agreement with the results reported for EPR studies of the interaction of BSA with vanadyl ion[25] and others metal ions such as gold(III)[55] and ruthenium(III).[56] In addition, it was suggested that strong interactions would be expected at pH 7 between vanadyl cation and BSA taking into account their association constant.[57]

As it is evident from our infrared analysis, the main conformational changes in BSA structure produced by the interaction with VO^{2+} were in agreement with the results obtained for HSA/oxovanadium(IV) complexes, though vanadyl species seemed to produce more significant perturbations in BSA than in HSA.[58]

Figure 2C shows the second derivative of BSA/VO_3^- complexes spectrum and the curve fitting performed on the original complex spectrum carried out as indicated in Section 4.1. This quantitative analysis of the secondary structure yielded a 72% of α-helix conformation, which corresponded to the strong and broad band at 1654 cm^{-1} displayed by the second derivative spectrum. The other contributions to the secondary structure are indicated in Table 1 and were calculated considering the following minimums: 1675 cm^{-1} for β-antiparallel, 1639 cm^{-1} for random coil and 1616 cm^{-1} for β-sheet structures. It is important to note that these latter bands had a minor contribution to the secondary structure of BSA in the presence of BSA/VO_3^- species. Furthermore, the absence of the 1630 cm^{-1} is indicating strong structural changes involving the loss of solvated helix and the feasible formation of compact hydrophobic cores in BSA/VO_3^- complexes.[33,46] Therefore, our FT-IR results indicated that when the interaction between BSA and VO_3^- species takes place, a significant increase in α-helix conformation occurs, which allows us to assume a greater folding of BSA with reduction in the hydration of the protein and an enhancement in the hydrophobic interactions in the core of BSA molecule.

As regards BSA/VO_3^- interaction studied by UV–Vis spectroscopy, it was rather difficult to be performed due to a superimposition of a free vanadate typical band with λ_{max} at 266 nm[59] with the BSA band at 278 nm increasing the intensity in the BSA/vanadate spectra.

An overview of our results obtained for BSA/VO_3^- complex lead us to attribute them to the size of the bonding ion. Makino et al.[60] have demonstrated the importance of the ion size in incrementing α-helix conformation. They have reported for other ions such as perchlorate, Mg(II), and Na(I) that α-helix proportion increased and a high stabilization was produced due to the ion size.

2.2. FT-Raman spectroscopy

In order to get a deeper insight into the BSA conformation changes when it interacts with vanadium species and to confirm FT-IR and UV–Vis spectroscopy results, Raman spectroscopy was performed on native BSA and the corresponding vanadium species complexes. Raman spectroscopy has emerged as a valuable tool to study conformational changes in proteins. Amide I (near 1650 cm^{-1}) and Amide III (near 1250 cm^{-1}), regions can provide information on the peptide backbone and have been used to assign secondary structures in proteins.[29,31,61–63] In addition, some details of protein ter-

tiary structure (environment of tyrosine side chain, disulfide bridge conformations, hydrophobic interactions, salt bridges) can also be revealed by this technique.[29,32,64–68]

To facilitate the study of the interaction between vanadium species and BSA, the secondary structure analysis in Amide III region was performed with FT-Raman spectra of BSA, BSA/VO^{2+}, and BSA/VO_3^- complexes. As it was found in our FT-IR spectroscopy results this interaction could be detectable in FT-Raman spectra if vanadium species concentration was higher than 0.5 M (data not shown). Figure 4 and Table 2 show band intensities of the major components (α-helix, random coil, and β-sheet) of Amide III region in vector normalized spectra of BSA, BSA/VO^{2+}, and BSA/VO_3^-. BSA spectra displayed higher intensity at the bands assigned to α-helix conformation (1280–1270 cm^{-1}) with a minor contribution of β conformation (1235–1225 cm^{-1}) and random coil structure (1265–1240 cm^{-1}). By means of FT-Raman spectroscopy it was possible to study how BSA underwent a conformational change from ordered structures to random coil when it was incubated with vanadyl salts. This protein unfolding was indicated in BSA/VO^{2+} spectra as a broad band with a relatively high intensity in the region assigned to random coil conformation, with respect to the same band for native BSA and BSA/VO_3^- spectra. On the other hand, a high intensity in the band assigned to α-helix conformation was found in BSA/VO_3^- complex spectra with a lower intensity for the bands assigned to random coil and β-structures (Fig. 4 and Table 2). Although an accurate quantitative analysis of α-helix, β-type structures, and random coil contributions is not allowed to be performed by FT-Raman, the results shown in Figure 4 and Table 2 are consistent with the results obtained by FT-IR/ATR spectroscopy displayed in Table 1.

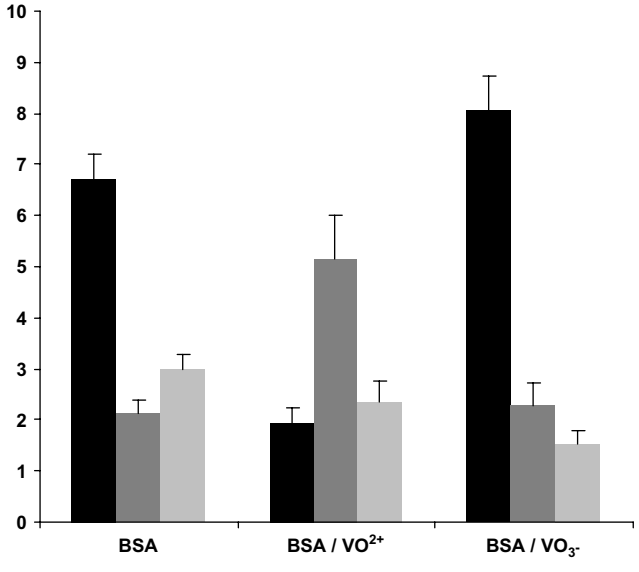

Figure 4. Band Intensity calculated in Amide III region with vector normalized in the whole range (4000–500 cm^{-1}) spectra. Baseline was corrected as indicated in methods. ■ α-helix (1280–1270 cm^{-1}), ■ random coil (1265–1240 cm^{-1}), and ■ β-sheet (1235–1225 cm^{-1}) contributions. Standard errors are indicated with bars.

Table 2. Raman shifts in free BSA, BSA/VO^{2+}, and BSA/VO_3^- complexes in Tris–HCl buffer solutions[a]

Raman shifts frequencies (cm^{-1})			Tentative assignments[b]
BSA	BSA/VO^{2+}	BSA/VO_3^-	
503 (w)	503 (w)	503 (w)	SS
830 (w)	831 (w)	831 (w)	Tyr buried
852 (w)	853 (w)	853 (w)	Tyr exposed
937 (m)	937 (m)	937 (m)	CC
970 (nd)	970 (w)	970 (nd)	V=O
1004 (s)	1004 (s)	1004 (s)	Phe
1250 (m)	1255 (m)	1257 (m-s)	Amide III
1270 (m)	1270 (m-s)	1274 (m)	
1386 (w)	1393 (w)	1388 (w)	CO_2^-
1403 (w)	1404 (w)	1403 (w)	
14445 (s)	1442 (s)	1442 (s)	CH_2
1456 (w,sh)	1454 (w, sh)	1454 (w, sh)	
1552 (w)	1548 (w)	1546 (w)	Amide II
1657 (s)	1660 (w, broad band)	1657 (s)	Amide I

[a] Free BSA solution in 2% w/v in Tris–HCl buffer (0.1 M, pH 7.4) and BSA/VO^{2+} and BSA/VO_3^- complexes were produced in Tris–HCl buffer solutions with [BSA] = 2% w/v, and [VO^{2+}] = 0.5 mM or [VO_3^-] = 0.5 mM, respectively. Letters in parentheses 'w', 'm', 's', and 'nd' mean relative intensities, 'weak', 'medium', and 'strong', and 'not detected', respectively, while 'sh' denotes that the peak constitutes a shoulder of a band.

[b] Band assignment was performed taking into account Refs. 29, 30, 35, 47 and 72.

2.2.1. Tyrosine doublet. One of the significant changes observed in BSA Raman spectra when BSA was incubated with vanadium species was in the lines assigned to the aromatic-side chain vibrations of tyrosine groups. The detected changes indicated that the microenvironments of tyrosyl groups were greatly altered by the interaction of BSA with vanadium ions. The ratio of the tyrosyl doublet around 850 and 830 cm^{-1} ($I_{850/830}$) is known as a good indicator of the hydrogen bonding of the phenolic hydroxyl group. A decrease of $I_{850/830}$ ratio was reported to reflect an increase in buriedness suggesting possible involvement of tyrosyl residues in intermolecular interactions.[29] When tyrosine residues are exposed, the 850 cm^{-1} band becomes more intense than the 830 cm^{-1} band.[29] The $I_{850/830}$ value calculated for BSA/VO^{2+} complexes was significantly higher than the value obtained for BSA/VO_3^- complexes (1.82 ± 0.05 vs 0.59 ± 0.01) indicating that in BSA/VO^{2+} complexes a higher number of tyrosine groups could be exposed to the surface of the protein (Fig. 5A). These results would be due to the disruption of the α-helix conformations and the enhanced in random coil structure that occurred in BSA/VO^{2+} complexes, demonstrated by the analysis of Amide I and III by ATR-FT-IR and Raman spectroscopy, respectively. On the other hand, for BSA/VO_3^- complexes spectra the intensity of the peak assigned to buried tyrosine was 0.44 ± 0.02 compared to 0.25 ± 0.01 for BSA/VO^{2+} complexes (Fig. 5A). The secondary structure of BSA/VO_3^- complexes was characterized by a high contribution of α-helix conformation (70%), and then tyrosil groups

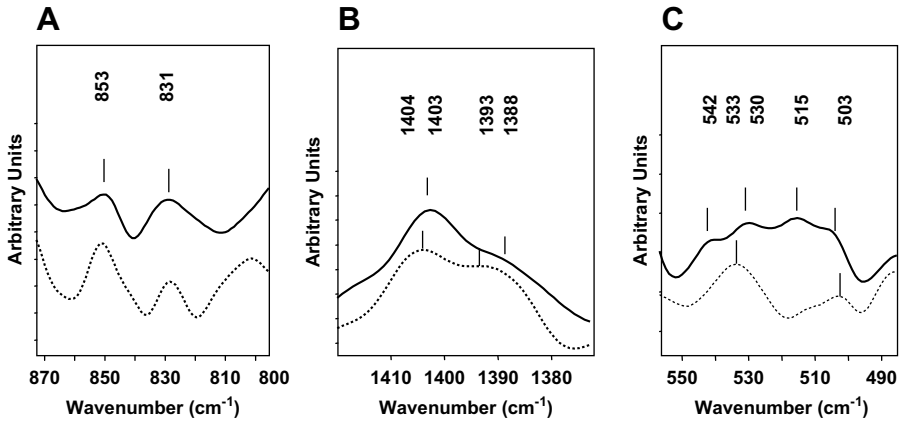

Figure 5. FT-Raman spectra of —— vanadate (BSA/VO_3^-) and …… vanadyl (BSA/VO^{2+}) complexes, obtained from freeze–dried power. Spectra were vector normalized in the whole range. (A) Tyrosine doublet (B) carboxylate vibration modes indicating charged side chains and salt bridging, and (C) disulfide bridges.

might be mainly evolved in the interaction among α-helix segments.

2.2.2. Charged side chains and salts bridging. Spectral features of carboxylate salt bridges were studied by means of 1410 and 1386 cm^{-1} band frequencies attributed to the COO^- vibrational mode which up shifts when salt bridge disruption is produced.[37,72] In fact, it was well established that COO^- bands shift to higher frequencies as the interactions of COO^- groups with their oppositely charged partners weakened (mainly Arg and Lys).[72] The FT-Raman vector normalized in the whole range spectra showed an up shift of the 1386 cm^{-1} band to 1388 cm^{-1} for BSA/VO_3^- and 1393 cm^{-1} for BSA/VO^{2+} complexes that could be interpreted in terms of salt bridge disruption (Fig. 5B). In the case of BSA/VO^{2+} complexes, two main factors could be contributing: the disruption of salt bridges due to the enhanced in random coil conformation, and a possible disruption of the normal salt bridges as a result of a change in the oppositely charged partners (Lys or Arg) that could be replaced by VO^{2+} cations and lead to changes in the normal salts bridges and the corresponding Raman spectral bands. In the case of BSA/VO_3^- complexes, the negative species (VO_3^-) could also be interfering with the normal partners of COO^- as the side chains of Lys or Arg producing changes in the typical spectral signals of salt bridges.

2.2.3. Disulfide bridges. Disulfide bridges are important elements that add to the stability of the entire molecular structure of the protein.[29,72] Raman spectroscopy provides the only direct way of analyzing disulfide bonds. Our results showed that as it was previously described for BSA, the 18 disulfide groups have a typical S–S frequency at 503 cm^{-1} assigned to the gauche–gauche–gauche (g–g–g)[29] conformation (data not shown). For BSA/VO^{2+} complexes two fairly broad bands were observed, one at 503 cm^{-1} and the other centered at 533 cm^{-1} (Fig. 5C). BSA/VO_3^- complexes spectra, on the other hand, showed a very broad band in the region of 550–500 cm^{-1} with four main peaks, 503, 515, 530, and 542 cm^{-1}, suggesting that significant changes in the geometry of the CSSC dihedral angles were produced in BSA conformation when incubated with VO_3^- species.

3. Summary and conclusions

The present data show that the native conformation of BSA is affected when it is incubated with both bioactive VO^{2+} and VO_3^- species. As regards BSA/VO^{2+} complexes a substantial increase in random coil conformation, a higher exposure of tyrosine groups, a significant disruption of salt bridging sites, and conformational variations of disulfide bonds were the main structural changes observed in comparison with BSA structure. In contrast, BSA/VO_3^- complexes showed a significant change in secondary structure conformation but with a substantial increase of α-sheet structure (pointing to a more ordered structure). Additionally, though in a minor proportion than oxovanadium(IV) complexes, salt bridging sites were disrupted with a higher exposition of tyrosine residues. Finally, conformational variations of disulfide bonds were detected for BSA/VO_3^- complexes in comparison with BSA structure. Also the relevance of the role of the vanadate anion (esspecially its size) could be related to its ability to bind BSA protein.

Therefore, this study clearly shows that the spectroscopic techniques FT-IR, FT-Raman, and UV–Vis spectroscopies used in a complementary way as they have been applied in this work enabled the direct detection of significant structural changes in BSA secondary and tertiary structure when incubated with vanadium species. Furthermore, a detailed secondary structural conformation analysis of BSA, BSA/VO^{2+}, and BSA/VO_3^- complexes could be performed. Former studies have been focused on the effects in the coordination mode of the vanadyl complexes. Not much investigation has been carried out in order to study the structural and conformational modifications in the protein after the metal binding. The results obtained herein might help to provide more evidences on the mode of action of the vanadium species interacting with the BSA plasma protein.

As it is mentioned above, the results obtained for vanadyl are consistent with those for the interaction of positive ions, though oxovanadium species seem to cause stronger perturbation on BSA than observed for HSA.

The understanding of the different structural changes that vanadyl and vanadate species produced in BSA structure could serve for a better knowledge of the mechanism that is involved in the therapeutic action of organic vanadium complexes, which denote different and relevant biological activities (e.g., insulin mimetic and anticarcinogenic properties).

4. Experimental

4.1. Materials and methods

4.1.1. Protein and complex preparation. Bovine serum albumin BSA (A-6003, essentially fatty acid-free) was obtained from Sigma Chemical Company (St. Louis, MO) and used as supplied. The $VOCl_2{\cdot}2H_2O$ (Carlo Erba) and $NaVO_3$ (Aldrich) salts used were of analytical grade. These drugs were selected considering that chloride and sodium are the most abundant ions in plasma. BSA was dissolved in Tris–HCl (0.1 M, pH 7.4) buffer to attain a final concentration of 4% w/v (~0.6 mM). Vanadium salt solutions were added drop wise to the 2% BSA solution (~0.3 mM) with constant stirring to ensure the formation of homogeneous solution and to obtain the desired metal ion concentration of 0.005, 0.05, and 0.5 mM. The BSA concentration used in this study is the one usually applied in metal–albumin interactions (e.g., human serum albumin is about 0.63 mM (40 mg/ml) in blood). Three independent replicates of BSA solutions, BSA/VO^{2+}, and BSA/VO_3^- complexes were performed. Solutions were allowed to stand for 1 h before being placed on the ATR cells. These solutions were also assayed by UV–Vis electronic spectroscopy. In order to improve signal–noise ratio in Raman spectra, Tris–HCl buffer, BSA solutions, and BSA/vanadium complexes were lyophilized. This procedure was carried out taking into account that as occurred with other proteins, particularly globulins, FT-Raman spectra of protein solutions and freeze–dried powders are almost identical, therefore, freeze drying do not affect protein conformation as determined by FT-Raman spectroscopy.[29,37,69]

4.1.2. Spectroscopic measurements and data processing

4.1.2.1. FT-IR spectroscopy. FT-IR/ATR spectra were recorded with a Bruker IFS 66 FTIR-spectrophotometer from 4000 to 400 cm^{-1} equipped with an internal reflectance accessory using ZnSe crystal designed to have one angle of light incidence of 45°. Spectra were recorded at room temperature with a spectral resolution of 4 cm^{-1}. To improve the signal-to-noise ratio, 200 scans were averaged for each spectrum. As most available published peak tables commonly contain and refer to transmission spectra, peak positions, absorbance intensities, and overall spectral patterns were corrected by ATR correction algorithms. Spectra of the Tris-buffer were subtracted from protein solution and protein–vanadium species prior to obtaining the second derivative spectra in a similar procedure described in the literature.[28] A good subtraction was obtained by a flat baseline around 2200 cm^{-1} caused by the cancellation of the water combination mode (1600 + 600 cm^{-1}). Several control tests with the same protein and metal ion solutions were made in order to obtain a flat baseline.[70] The results were reported as averages of the three independent replicates. For each treatment the corresponding average spectra (Xm) and standard deviation (σ) were calculated using Opus software. For the analysis of differences among treatments Xm ± 2σ were taken into account (confidence limit 97.7%) (OPUS, Bruker Optics, USA).

4.1.2.2. Determination of protein secondary structure. Determination of secondary structure of BSA and BSA/vanadium complexes was carried out on the basis of the procedure described by Byler and Susi.[71] The Amide I region (1700–1600 cm^{-1}) was used to investigate the secondary structure of BSA in aqueous solution in a quantitative manner. The frequencies, the number of peaks to be fitted, and the half-width of each peak to start a least-square iterative curve-fitting procedure were those obtained from the second derivative of the original spectra. The areas of the bands were calculated by integration of the corresponding fitted band. A straight baseline passing through the ordinates at 1700 and 1600 cm^{-1} was adjusted as an additional parameter to obtain a best fit. The curve-fitting procedure was performed by stepwise iterative adjustment towards a minimum root-mean-square error of the different parameters determining the shape and position of the absorption peaks. It was carried out by assuming an initial mixed Lorentzian–Gaussian line-shape function, with full width band at half-height (FWHH) of 13–18 cm^{-1} and a maximum resolution factor. Base line corrections, normalization, derivation, curve fitting and area calculation were carried out by means of Grams/32 (Galactic Industries Corporation, USA) software, OPUS 3.1 and Perkin-Elmer software. The resulting fitted curve was analyzed taking into account the band assignment for the secondary structure previously reported in the literature,[6] α-helix, 1658–1650 cm^{-1}; β-sheets, 1637–1613 cm^{-1}; turns, 1673–1666 cm^{-1}; random coil, 1645–1637 cm^{-1}; and β-antiparallel, 1695–1675 cm^{-1}. In order to calculate the percentage contribution of the different types of conformations to the area of all the components, bands assigned to a given conformation were summed and divided by the total Amide I area.[48] The obtained number was taken as the proportion of the polypeptide chain in the corresponding conformation.

4.1.2.3. UV–Vis spectroscopy. Electronic absorption spectra were recorded with a Hewlett–Packard 8453 diode-array spectrophotometer, using 1 cm quartz cells in the range (200–800 nm). Buffer solutions were placed in the reference compartment. Three independent replicates of BSA suspension and the corresponding complexes were measured.

4.1.2.4. FT-Raman spectroscopy. Raman spectra were collected on a Bruker IFS 113 FT-IR spectrophotometer provided with the NIR Raman attachment equipped with an Nd:YAG laser at 1064 nm laser. Frequency calibration of the instrument was undertaken using the sulfur line at 217 cm^{-1}. Spectra were recorded at room temperature with a laser power of 500 mW, and spectral

resolution of 4 cm^{-1}. Each spectrum was obtained after collecting and averaging 2000 scans in order to obtain high signal-to-noise ratio spectra. FT-Raman spectra were plotted as intensity (arbitrary units) against Raman shift in wavenumber (cm^{-1}). All spectra were vector normalized in the whole range (4000–500 cm^{-1}). The plotting, processing, normalizations, manipulations, and evaluation of spectra were carried out through OPUS software (Bruker Optics, Germany). Buffer spectra were recorded with the same instrument settings employed for protein solutions and when it was necessary, bands were further compensated by computer subtraction techniques (Opus software). Band intensities were calculated after a linear baseline correction performed with an integration method developed within OPUS software. Particularly, in Amide III region, peak intensities were calculated in the range 1280–1200 cm^{-1} setting up two different baselines: (1) a straight line connecting 1280 with 1230 cm^{-1} for the calculation of α (near 1277 cm^{-1}) and random coil (near 1248 cm^{-1}) contributions, and (2) another straight line connecting 1230 with 1200 cm^{-1} for the calculation of peak intensity associated to β-sheet contribution (near 1231 cm^{-1}). The intensity values obtained for the tyrosine doublet were calculated relative to the local baseline of each peak (830 and 850 cm^{-1}). Band assignment of the major vibrational motions of the side chains or the peptide backbone was based on comparison to Raman data reported in the literature.[29,30,35,47,72] All analyses were performed in three independent experiments, and the results were reported as averages of these replicates.

Acknowledgments

We highly appreciate the financial supports received from UNLP and CONICET (PIP-5078). E.G. Ferrer and E.J. Baran are members of the Carrera del Investigador, CONICET. A. Bosch is a member of the Carrera del Investigador CICPBA, Argentina. The authors thank Dr. Patricia A.M. Williams and Dr. Susana B. Etcheverry for kindly correcting this manuscript.

References and notes

1. Nonaka, M.; Li-Chan, E.; Nakai, S. *J. Agric. Food Chem.* **1993**, *41*, 1176.
2. Goodman, D. S. *J. Am. Chem. Soc.* **1958**, *80*, 3892.
3. Adams, P. A.; Berman, M. C. *Biochem. J.* **1980**, *191*, 95.
4. Yamashita, M. M.; Wesson, L.; Eisenman, G.; Eisenberg, D. *Proc. Natl. Acad. Sci. U.S.A.* **1990**, *87*, 5648.
5. Bal, W.; Christodoulou, J.; Sadler, P. J.; Tucker, A. *J. Inorg. Biochem.* **1998**, *70*, 33.
6. Rawel, H. M.; Rohn, S.; Kruse, H. P.; Kroll, J. *Food Chem.* **2002**, *78*, 443.
7. Zhang, Y.; Wilcox, D. E. *J. Biol. Inorg. Chem.* **2002**, *7*, 327.
8. Harford, C.; Sarkar, B. *Acc. Chem. Res.* **1997**, *30*, 123.
9. Macara, I. G. *Science* **1980**, *5*, 92.
10. Rehder, D. *Biometals* **1991**, *5*, 3.
11. Tsiani, E.; Fantus, I. G. *Trends Endocrinol.* **1997**, *8*, 51.
12. Byczkowski, L. Z.; Wan, B.; Kulkarni, A. P. *Bull. Environ. Contam. Toxicol.* **1988**, *41*, 696.
13. Carmichael, A. J. *FEBS Lett.* **1990**, *261*, 165.
14. Ozawa, T.; Hanaki, A. *Chem. Pharm. Bull.* **1989**, *37*, 1407.
15. Sakurai, H.; Fujii, K.; Fujimoto, S.; Fujisawa, Y.; Takechi, K.; Yasui, H. In *Vanadium Compounds: Chemistry, Biochemistry and Therapeutic Applications*; Tracey, A. S., Crans D. C., Eds.; ACS Symposium Series; New York, 1998; Vol. 711, pp 344.
16. Vanadium in the Environment. In *Adv. Environ. Sci. Technol*; Nriagu, J. O., Ed; John Wiley and Sons Inc.: New York, 1998; Vol. 31, part 2 (Health Effects).
17. Vanadium in the Environment. In *Adv. Environ. Sci. Technol*; Nriagu, J. O., Ed; John Wiley and Sons Inc.: New York, 1998; Vol. 30, part 1 (Chemistry and Biochemistry), Chapter 12, pp 285.
18. Baran, E. J. In *Vanadium in the Environment*; Nriagu, J. O., Ed.; John Wiley and Sons: New York, 1998, part 2 (Health Effects) Chapter 16, pp 317.
19. Rehder, D. *Inorg. Chem. Commun.* **2003**, *6*, 604.
20. Sakurai, H.; Tamura, A.; Fugono, J.; Yasui, H.; Kiss, T. *Coord. Chem. Rev.* **2003**, *245*, 31.
21. Makinen, M. W.; Brady, M. J. *J. Biol. Chem.* **2002**, *277*, 12215.
22. Nechay, B. R. *Ann. Rev. Pharmacol. Toxicol.* **1984**, *24*, 501.
23. Toshikazu, H. *Chem. Rev.* **1997**, *97*, 2707.
24. Heinemann, G.; Fichtl, B. l.; Mentler, M.; Vogt, W. *J. Inorg. Biochem.* **2002**, *90*, 38.
25. Chasteen, N. D.; Francavilla, J. *J. Phys. Chem.* **1976**, *80*, 867.
26. Liborion, B. D.; Thompson, K. H.; Hanson, G. R.; Lam, E.; Aebischer, N.; Orvig, C. *J. Am. Chem. Soc.* **2005**, *127*, 5104.
27. Dörnyei, Á. D.; Marcão, S. M.; Costa Pessoa, J.; Jakusch, T.; Kiss, T. *Eur. J. Inorg. Chem.* **2006**, *18*, 3614.
28. Susi, H.; Byler, D. M. *Biochem. Biophys. Res. Commun.* **1983**, *115*, 391.
29. Tu, A. T. Raman Spectroscopy in Biology. In *Principals and Applications*; John Wiley and Sons Inc.: New York, 1982.
30. Li-Chan, E. C. Y. In *Methods to Monitor Process-induced Changes in Food Proteins. An overview. Process—Induced Chemical Changes in Foods*; Shahidi, F., Ho, C.-T., Chuyen, N., Eds.; New York, 1998, pp 5.
31. Williams, W.; Dunker, A. K. *J. Mol. Biol.* **1981**, *152*, 783.
32. Overman, S. A.; Thomas, G. J., Jr. *J. Raman Spectrosc.* **1998**, *29*, 23.
33. Fabian, H.; Mäntele, W. In *Infrared Spectroscopy of Proteins. Handbook of Vibrational Spectroscopy*; Chalmers, J. M., Griffiths, P. R., Eds.; Biochemical Applications; John Wiley and Sons Ltd: Chichester, 2002; p 3399.
34. Fabian, H.; Schultz, C. P. In *Fourier Transform Infrared Spectroscopy in Peptide and Protein Analysis*; Meyer, R. A., Ed.; Encyclopedia of Analytical Chemistry; John Wiley and Sons: Chichester, 2000; p 5779.
35. Ma, C. Y.; Phillips, D. L. *Cereal Chem.* **2002**, *79*, 171.
36. Casal, H. L.; Kohler, U.; Mantsch, H. H. *Biochim. Biophys. Acta* **1988**, *957*, 11.
37. Li-Chan, E.; Nakai, S.; Hirotsuka, M. In *Raman Spectroscopy as Probe of Protein Structure in Food Systems*; Yada, R. Y., Jackson, R. L., Smith, L. L., Eds.; Protein Structure–Function Relationship in Foods; Blakie Academic: London UK, 1994; p 163.
38. Meng, G.; Ma, C. Y.; Phillips, D. L. *Food Chem.* **2003**, *81*, 411.
39. Ma, C. Y.; Rout, M. K.; Mock, W. Y. *J. Agric. Food Chem.* **2001**, *49*, 3328.
40. Fringeli, U. P. In *In situ Infrared Attenuated Total Reflection Membrane Spectroscopy*; Mirabella, F. M., Ed.; Internal Reflection Spectroscopy, Theory and Applications; Marcel Dekker: New York, 1992; p 255.

41. Goormaghtigh, E.; Raussens, V.; Ruysschaert, M. M. *Biophys. Acta* **1999**, *1422*, 105.
42. Gilmanshin, R.; Williams, S.; Callender, R. H.; Woodruff, W. H.; Dyer, R. B. *Proc. Natl. Acad. Sci. U.S.A.* **1997**, *94*, 3709.
43. Surewicz, W. K.; Mantsh, H. H.; Chapman, D. *Biochemistry* **1992**, *32*, 389.
44. Tamm, L. K.; Taulian, S. A. *Q. Rev. Biophys.* **1997**, *30*, 365.
45. Carter, D. C.; He, X. M.; Munson, S. H.; Twigg, P. D.; Gernert, K. M.; Broom, M. B.; Miller, T. Y. *Science* **1989**, *244*, 1195.
46. Murayama, K.; Tomida, M. *Biochemistry* **2004**, *43*, 11526.
47. Damain, G.; CapeanRomanian, V. *J. Biophys.* **2005**, *15*, 67.
48. Lippert, J. L.; Tyminski, D.; Desmeules, P. J. *J. Am. Chem. Soc.* **1976**, *98*, 7075.
49. Ahmed, A.; Tajmir-Riahi, A. *J. Inorg. Biochem.* **1993**, *50*, 235.
50. Kanthinathi, M.; Maheshwari, R.; Chathathreyan, D. *Lamgmuir* **2003**, *19*, 3398.
51. Stoscheck, C. M. *Methods Enzymol.* **1990**, *182*, 50.
52. Ballhausen, C. J.; Gray, H. B. *Inorg. Chem.* **1962**, *1*, 111.
53. Dessì, A.; Micera, G.; Sanna, D. *J. Inorg. Biochem.* **1993**, *52*, 275.
54. Liang, H.; Huang, J.; Tu, C. Q.; Zhang, M.; Zhou, Y. Q.; Shen, P. W. *J. Inorg. Biochem.* **2001**, *85*, 167.
55. Marcon, G.; Messori, L.; Orioli, P.; Cinellu, M. A.; Ghetti, G. *Eur. J. Biochem.* **2003**, *270*, 4655.
56. Messori, L. L.; Orioli, P.; Vullo, D.; Alessio, E.; Lengo, E. *Eur. J. Biochem.* **2000**, *267*, 1206.
57. Vanadium and its Role in Life. In *Metal Ions in Biological Systems*; Sigel, H., Sigel, A., Eds.; Chasteen N. D. in Vanadium–Protein Interactions; Marcel Dekker Inc.: New York, 1995, Vol. 31, Chapter 7, pp 235.
58. Purcell, M.; Neault, J. F.; Malonga, H.; Arakawa, H.; Tajmir-Riahi, H. A. *Can. J. Chem.* **2001**, *79*, 1415.
59. Harris, W. R.; Carrano, C. J. *J. Inorg. Biochem.* **1984**, *22*, 201.
60. Makino, S.; Wakabayashi, K.; Sugai, S. *Biopolymers* **1968**, *6*, 551.
61. Pelton, J. T.; McLean, L. R. *Anal. Biochem.* **2000**, *277*, 167.
62. Williams, W. *J. Mol. Biol.* **1983**, *166*, 581.
63. Alix, A. J. P.; Pedanou, G.; Berjot, M. J. *Mol. Struct.* **1988**, *174*, 159.
64. Overman, S. A.; Thomas, G. J., Jr. *Biochemistry* **1998**, *37*, 5654.
65. Overman, S. A.; Thomas, G. J., Jr. *Biochemistry* **1999**, *38*, 4018.
66. Tsuboi, M.; Suzuki, M.; Overman, S. A.; Thomas, G. J., Jr. *Biochemistry* **2000**, *39*, 2677.
67. Carmnona, P.; Molina, M.; Rodíguez-Casado, A. *Eur. Biophys. J.* **2003**, *32*, 137.
68. Chang, J.; Ballatore, A. *FEBS Lett.* **2000**, *473*, 183.
69. Ma, C. Y.; Rout, M. K.; Chan, W.; Phillips, D. L. *J. Agric. Food Chem.* **2000**, *48*, 1542.
70. Nonaka, M.; Li-Chan, E.; Nakai, S. *J. Agric. Food Chem.* **1993**, *41*, 1176.
71. Byler, D. M.; Susi, H. *Biopolymers* **1986**, *25*, 469.
72. Ngarize, S.; Herman, H.; Adams, A.; Howell, N. K. *J. Agric. Food Chem.* **2003**, *52*, 6470.